Transactions on Energy Systems and Engineering Applications

Article

High-speed 3D optical sensing for manufacturing research and industrial sensing applications

Beiwen Li[1,*]

[1] Department of Mechanical Engineering, Iowa State University, Ames, Iowa, 50011, USA.

[*] Correspondence: beiwen@iastate.edu

Received: 10 October 2022; Accepted: 19 November 2022; Published: 5 December 2022

Abstract: This paper presents examples of high-speed 3D optical sensing for research and applications in the manufacturing community. Specifically, this paper will focus on the fringe projection technique as a special technology that can be extremely beneficial to manufacturing applications, given its merits of simultaneous high-speed and high-accuracy 3D surface measurements. This paper will introduce the basic principles of 3D optical sensing based on the fringe projection technique as well as the enabled manufacturing research applications, including both in-situ/in-process monitoring and post-process quality assurance.

1. Introduction

In the coming era of Industry 4.0 and smart manufacturing, the importance of smart sensors and sensing systems has been increasingly emphasized [1]. The recent advances in machine/computer vision technologies have produced new smart sensors and sensing systems impacting different aspects of manufacturing processes. Three-dimensional (3D) optical sensing technologies, which add one more dimension on top of conventional imaging and vision technologies, will provide a much greater impact to scientists and researchers in the field of smart manufacturing, given their ability to digitize the scenes being viewed in 3D [2, 3, 4].

For manufacturing processes, 3D optical sensing could impact aspects ranging from in-process monitoring and diagnosis to post-process quality inspection. Conventionally, a 3D optical sensing system is mostly used for post-manufacturing part dimensional inspections with precision static 3D geometric profiling. As a nondestructive method, 3D optical sensing can significantly increase the inspection speed, and throughput of traditional contact methods such as stylus profilometers or coordinate measuring machines (CMM) [5, 6]. However, as smart manufacturing puts more emphasis on in-process decision-making and closed-loop control, conventional static 3D optical sensing may no longer satisfy the requirement, given that real-time data acquisition and processing are needed. Taking the advanced additive manufacturing

How to cite this article: Li, Beiwen. High-speed 3D optical sensing for manufacturing research and industrial sensing applications. *Transactions on Energy Systems and Engineering Applications*, 3(2): 490, 2022. DOI:10.32397/tesea.vol3.n2.490

technology as an example where in-process diagnosis plays a significant role, a real-time 3D optical sensing system can be extremely valuable if incorporated into the envelope of an additive printing machine to acquire the layer-by-layer surface topographies of the printed constructs [7, 8]. Achieving this, however, poses significant challenges for current 3D optical sensing techniques, given the combined requirements of high speeds and high accuracies for the measured 3D surface topographies.

Recent major advancements in computing power and graphics have drastically boosted the development of 3D optical sensing technologies [9, 10]. Capabilities (e.g., real-time measurements) that were barely even thought possible a few years ago are now being introduced into the field of 3D optical sensing. The 3D optical sensing approaches can be broadly divided into three major categories: interferometry, time-of-flight, and triangulation [11]. Interferometry [12, 13, 14] is by far the most accurate type of 3D optical metrology technique, which can achieve an accuracy as high as nanometers. However, interferometry typically has a limited range of measurements (e.g., at micrometer scale) and thus is typically used as a post-process inspection technology. Time-of-flight [15, 16, 17, 18] is a technique that emulates the echolocation of certain types of animals (e.g., a bat), where the depth or distance information is typically obtained by calculating the round-trip traveling time of emitted light source. This technology is generally well-suited for measuring a large scene (e.g., with a room size) and has been used in commercial products such as Microsoft Kinect V2 [19]. However, given the ultra-fast speed of light, it is difficult for the time-of-flight technology to detect a depth difference smaller than one millimeter, which can be vital to recognize small features on a surface. Triangulation-based approaches are the most suitable technology for measuring medium-scale objects (e.g., a length scale from 1 cm to 1 m). The three most well-known triangulation-based technologies include laser scanning [20, 21, 22, 23], stereo vision [24, 25] and structured light [26, 9, 10]. The laser scanning method performs line-by-line scanning to obtain the surface topography of the scene, whose performance can be reduced when trying to map a complicated surface containing fine-scale features. The stereo 3D vision method obtains the 3D information through correspondence matching and triangulation, yet the correspondence identification can be difficult when the imaged scene lacks rich features for stereo matching. The structured light 3D vision overcomes these limitations by performing simultaneous whole-area scanning with codified structured illumination. Specifically, the fringe projection method that uses continuous sinusoidal codifications has achieved real-time (e.g., 30 Hz) 3D imaging with tens of μm accuracy or higher [27, 28, 29]. Given its capability of characterizing small features with minimal time delay induced by 3D imaging and reconstruction, the fringe projection technique can be regarded as the most suitable technology for in-process monitoring and inspection for many manufacturing processes.

This paper will introduce the basics of high-speed 3D optical sensing and the perspectives of its related research and applications in the manufacturing community. Specifically, a major focus will be put on the high-speed fringe projection technique, given its capability of simultaneous high-speed and high-accuracy measurements. The perspectives on how high-speed and high-accuracy fringe projection-based 3D optical sensing could benefit the manufacturing research will also be introduced, including how one could use such technology for both in-situ/in-process monitoring and post-process quality assurance. Specifically, in-situ measurements of an additive manufacturing process (i.e., direct energy deposition) will be demonstrated as an example of in-situ/in-process monitoring; and examples of precision geometric profiling, morphological data analysis, and surface integrity characterizations will be demonstrated as practical cases for post-process quality assurance.

Section 2 introduces the theoretical foundations of high-speed 3D optical sensing, including the background and the basics of the fringe projection technique, the phase shifting technique as one of the most widely used fringe analysis techniques, and some challenges in applying the fringe projection technique for industrial practices. Section 3 introduces the related manufacturing research and applications,

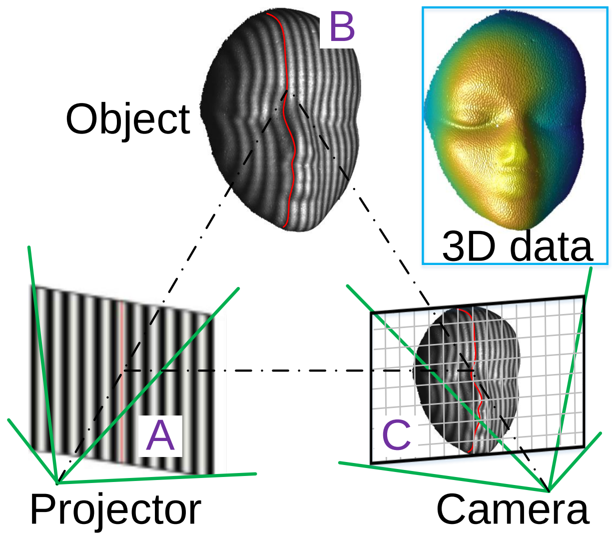

Figure 1. A schematic illustration of the fringe projection technique.

which include both in-situ/in-process monitoring and post-process quality assurance. Section 4 will serve as an executive summary of this paper.

2. Principles of high-speed 3D optical sensing

2.1. Basics of the fringe projection technique

3D optical techniques have achieved great success in medicine, virtual reality, tele-surgery, and many other disciplines. Optical means to perform high-speed 3D shape measurements are typically based on triangulation (e.g., stereo vision, spacetime stereo, laser scanning, structured light). The driving principle is to recover depth by matching and geometrically relating distinct regions of a scene viewed from different angles. The structured light approach, which hinges on the projection of known structured patterns onto objects, has brought increased attention because of its flexibility, speed, accuracy, and its ability to measure surfaces without strong natural features [30]. However, its spatial resolution is limited to being larger than a projector's pixel because of the need to encode artificial features using projector images [26].

The fringe projection technique is a variation of the structured light method where patterns with sinusoidally varying structures are illuminated. Sinusoidal structures have the advantage of being continuous and differentiable from neighboring pixels. Thus, high spatial resolutions at the camera-pixel-level can be achieved. Figure 1 shows a fringe projection system. The projector shines one-dimensional, sinusoidally varying stripes onto the sample object, and the camera captures the stripes distorted by the object's surface geometry. Fringe analysis techniques such as the phase shifting method (to be introduced next) are employed to identify the pixel-to-pixel correspondence between a projector point and a camera image point. Finally, the 3D coordinates are computed by the triangulation relationship between the projection unit (A), the 3D object (B), and the image acquisition unit (C).

2.2. The phase shifting technique

The key to a high-quality 3D reconstruction for the fringe projection technique is to select an accurate fringe analysis technique. Many fringe analysis methods were developed in the optics community, including the single-shot Fourier transform method [31] and the multi-shot phase shifting method [32]. For industrial measurements, the phase shifting technique is preferred compared to the Fourier transform method, given

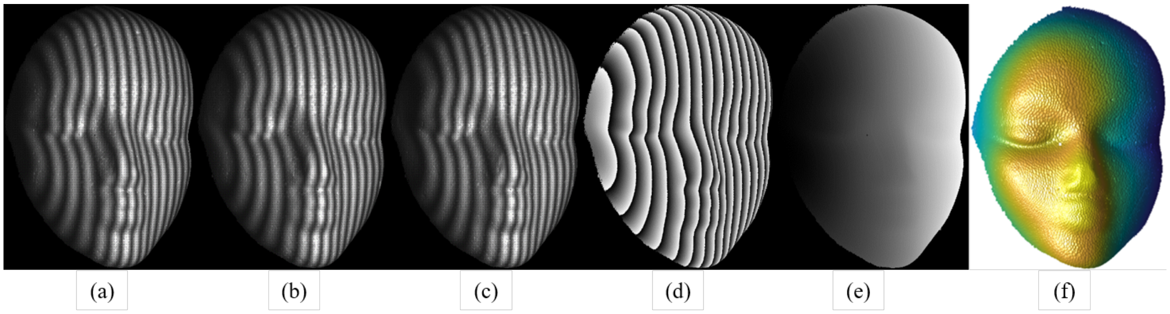

Figure 2. A demonstration of an example phase shifting process. (a) - (c) Example of three-step phase shifted fringe images; (d) wrapped phase map; (e) unwrapped phase map; (f) 3D geometry.

its ability better resolve the details of complex geometries. The basic principle of phase shifting is to project a set of sinusoidal patterns with equal phase shifts applied and then capture the corresponding camera images. The mathematical description of the phase-shifting method can be written as follows:

$$I_i(x,y) = I'(x,y) + I''(x,y)\cos(\phi + \delta_i), \tag{1}$$

where $I_i(x,y)$ denotes the $i-th$ captured fringe image as shown in Fig. 2(a) - 2(c) for a three-step ($i = 1,2,3$) phase shifting example; $I'(x,y)$ and $I''(x,y)$ respectively denote the average intensity and the intensity modulation; $\delta_i = 2i\pi/N$ denotes the phase shift added to the i-th fringe image. The phase map $\phi(x,y)$, which contains unique information regarding the object geometric profiles, can be obtained by solving simultaneous equations such that

$$\phi(x,y) = -\arctan\left[\frac{\sum_{i=1}^{N} I_i \sin(2i\pi/N)}{\sum_{i=1}^{N} I_i \cos(2i\pi/N)}\right]. \tag{2}$$

The solved phase map $\phi(x,y)$ naturally contains 2π discontinuities given the nature of the arctangent function, as shown in Fig. 2(d). To remove such discontinuity and obtain an absolute phase map, one can employ a temporal phase unwrapping method [33, 34] to obtain a final absolute continuous phase map $\Phi(x,y)$.

$$\Phi(x,y) = \phi(x,y) + k(x,y) \times 2\pi. \tag{3}$$

After obtaining the absolute continuous phase map $\Phi(x,y)$ as shown in Fig. 2(e), a phase-to-3D coordinate conversion can be performed by treating both the camera and the projector as pinhole imaging systems [35], and the sample result can be found in Fig. 2(f).

2.3. Challenges of fringe projection profilometry in industrial practices

To realize high-speed 3D imaging with fringe projection, it is crucial to achieve high speeds for both pattern projection and image acquisition. The advances in high-speed camera imaging technologies and high-speed image projection technologies (e.g., the digital-light-process technology) have pushed the speed limitation of the fringe projection technique to a capturing rate as fast as kilohertz with the help of bit-wise sinusoidal signal generation through projector defocusing [36]. In the meantime, the real-time processing speed of 3D reconstruction has been pushed to 30 Hz or more with the help of graphics processing unit [27, 28, 29]. However, to make the fringe projection technique generate impact for industrial practices, it is crucial to push the accuracy limit of this technology to industrial standards (e.g., a few micrometers) while maintaining a decent measurement speed suitable for in-situ applications.

One of the most important challenges for adopting the fringe projection technique in industrial or manufacturing applications is the difficulty in measuring metallic surfaces. This is because metallic surfaces are shiny and highly reflective in nature, which tends to generate a strong glare in camera images. Although there are many high-dynamic-range (HDR) methods developed to address this challenge [37, 38], it is still quite difficult even for the most advanced HDR fringe projection method to approach the high measurement accuracies that a conventional fringe projection method can achieve when measuring a white matte surface finish. In addition, the existence of dynamic motions in some operating manufacturing machines could make the situation even worse. Therefore, research opportunities are present in this area, and potential solutions may be sought by incorporating advanced machine learning technologies for accuracy enhancement in metallic surface measurements [39, 40].

Another important challenge is the measurement of large structures in manufacturing practices. Currently, the field of view of a single 3D scan using fringe projection is only around $1m^2$, scaling up this field of view will bring significant value in many manufacturing applications, such as the inspection of large manufactured parts or the generation of a full virtual representation of a manufacturing facility for digital twin modeling. Despite the advances in relevant technologies such as multi-view scanning and panoramic 3D point cloud stitching, it is still quite challenging to finish the whole scanning process and robustly create full 3D representations of a large manufacturing structure (with several meters of length/width) within minutes to hours even with the most advanced fringe projection technique. Given this, opportunities are present to combine robotic technologies with fringe projection and computer vision technologies for rapid 3D scans and digital modeling such that a full virtual representation of a manufacturing structure can be established automatically within a relatively short period.

3. Some related manufacturing research and applications

This section shows some representative manufacturing research and applications that were induced by fringe projection-based high-speed 3D optical sensing.

3.1. In-situ/in-process monitoring

Given the capability of refreshing fringe pattern images at a rate of 120 Hz or more (equaling a 3D acquisition rate of 40 Hz or more) with digital-light-processing projectors nowadays, the fringe projection-based 3D optical sensing technology has a high potential for applications related to in-situ/in-process monitoring of manufacturing processes. One of the most promising directions in this regard is to perform in-process monitoring for additive manufacturing processes. As identified in the field of additive manufacturing, one of the most important challenges is to perform real-time identification of defects such that one can decide to either stop the printing process or conduct corrective actions accordingly. Enabling this will pose a combined requirement of measurement speeds (i.e., close to real-time) and accuracies (i.e., at the micrometer level), providing research opportunities for the optics community.

Researchers have already attempted to employ fringe projection for in-situ monitoring of additive manufacturing processes such as laser powder bed fusion (LPBF) [41, 42, 43, 44] or direct energy deposition (DED) [45]. An example of using fringe projection for in-situ/in-process monitoring of a DED process by the author's research group [45] is shown in Fig. 3. Figure 3(a) shows the photograph of the physical 3D optical sensing system that was incorporated inside the envelope of a DED machine. The goal of this system setup is to monitor the surface topography printing results right after each surface layer is printed. Specifically, for this laboratory-made 3D optical sensing system, a FLIR Grasshopper Monochrome camera (Model: GS3-U3-23S6M-C) and a telecentric lens (Opto-engineering TC4MHR036-C with a magnification of 0.487) is used as the image acquisition unit. A digital-light-processing projector (Wintech 4500) was used as the pattern projection device. The camera and projector resolutions were 1280×960 and 912×1140,

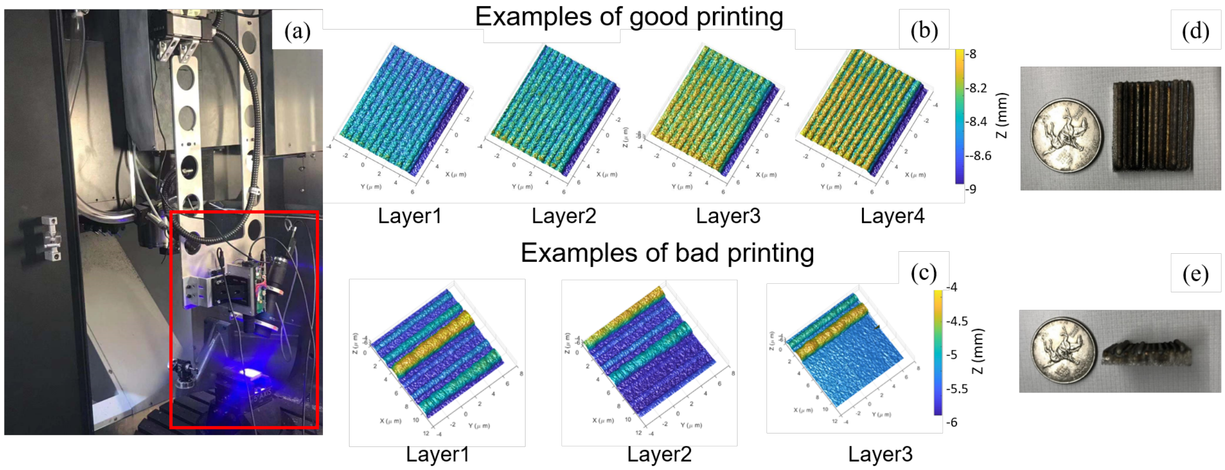

Figure 3. An in-situ 3D optical sensing system developed for in-process monitoring of direct energy deposition (DED) at Iowa State University. (a) The 3D optical sensing system incorporated inside the envelope of a DED machine; (b) the layerwise surface topography data for an example of good printing; (c) the layerwise surface topography data for an example of bad printing; (d) - (e) photographs of the bad printing samples with top view and side view, respectively.

respectively. To ensure a high-quality 3D acquisition, an 18-step phase shifting method ($N = 18$ in Eq. 2) is employed together with a gray-coding-based phase unwrapping strategy [46]. To avoid a nonlinear gamma calibration for projecting 8-bit grayscale images, squared binary patterns along with a slight projector defocusing [36] is applied to generate quasi-sinusoidal pattern profiles. The field-of-view of the entire 3D imaging system is slightly smaller than the printing area, so no background filtering is necessary.

Figure 3(b) - (c) respectively show examples of a good printing and a bad printing process, from which one can visualize that for a good printing process, the surface topography will show a uniform texture, yet abrupt curvature changes will exhibit in the bad printing sample. From this example measurement result, one can see the potential of using fringe projection-based 3D optical sensing for in-situ monitoring of an additive printing process, given that the high-speed nature of the fringe projection technique requires minimal time delay and interruption for the printing process.

3.2. Post-process quality assurance

3.2.1. Precision geometric profiling

For post-process quality assurance, the most straightforward application of 3D optical sensing is to perform precision geometric profiling for post-manufacturing dimensional inspection. Specifically, for the fringe projection technique, it has the capability to achieve accuracy at a 0.1 mm level with a one-meter length scale [35] or an accuracy of a few micrometers with a length scale of a few centimeters [47].

Figure 4 shows an example of using the fringe projection technique for precision geometric profiling of an industrial part (the inside of a hard disk). The system is composed of a FLIR Grasshopper Monochrome camera (Model: GS3-U3-23S6M-C) attached to a pinhole lens with a 12 mm focal length, as well as a digital-light-processing (DLP) projector (LightCrafter 4500). The camera and projector resolutions were 1280×960 and 912×1140, respectively. The same 3D reconstruction algorithms as used in the system shown in Fig. 3 (i.e., 18-step phase shifting, gray-coding-based phase unwrapping, and binary patterns with projector defocusing) were used in this application.

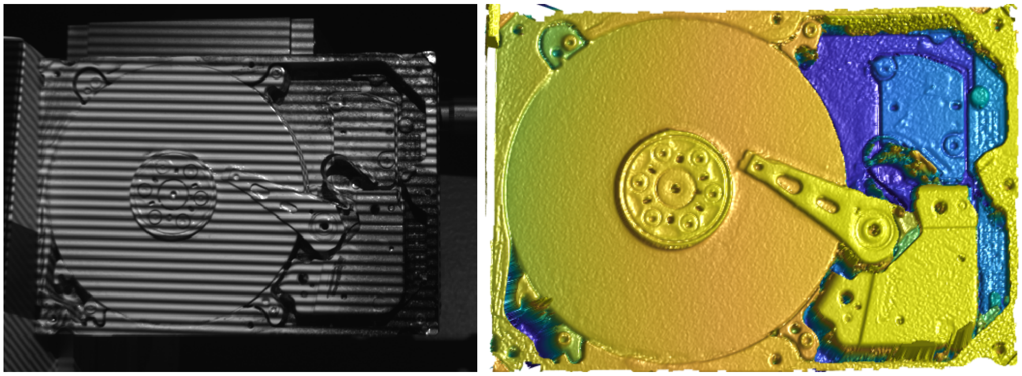

(a) (b)

Figure 4. An example 3D geometric measurement result of an industrial part using fringe projection. (a) The captured fringe image of a hard disk; (b) the corresponding reconstructed 3D result using the fringe image (a).

Figure 4(a) - 4(b) respectively show the captured camera fringe image with pattern projection and the corresponding reconstructed 3D geometric profile of the measured sample, from which one can see that the local fine-scale features (e.g., screws, flange, etc.) can be visualized on the reconstructed 3D geometry, showing the great potential of the fringe projection technique for rapid dimensional metrology and inspection for industrial parts.

3.2.2. Morphology data analysis

Once the geometric profiles are reconstructed through optical fringe analysis, some key dimensional features can be extracted through subsequent feature extraction such that a set of quality evaluation metrics can be established. An example of morphological data analysis application for a civil additive manufacturing process is shown in Fig. 5. In this application, the same system setup and the set of 3D reconstruction algorithms as used in the application in Section 3.2.1 was employed, except that only three-step phase shifting was used here ($N = 3$ in Eq. 2) due to its sufficient accuracy for measurements of non-metal surfaces.

Figure 5(a) shows the designed 3D solid model for clay additive printing, and Fig. 5(b) - (c) show different views of the actual printed structure. Figure 5(d) - (f) shows the reconstructed 3D geometries of three representative 3D printed samples prepared for quality evaluation. Specifically for this application, a set of evaluation metrics, including the deviations in layer width, layer thickness, height, outer diameter, cross-sectional area, and surface angle, were used for printing quality assessments, where the best printing quality is supposed to have the least deviations on these dimensions. Figure 5(g) shows the contour plots of the evaluation metrics for the three printed samples, from which one can see that the sample with the best visual quality (sample 1) has the least actual overall deviations. This application example demonstrates how one can use the 3D geometric data obtained from 3D optical sensing for morphological data analysis and quality assessments of manufactured products.

3.2.3. Characterization of surface integrity

Apart from the extraction of dimensional information, another type of important property that can be identified from 3D optical sensing is the surface integrity which contains important information regarding the areal surface or textural roughness information. An example of different surface textures produced by different DED printing parameters is shown in Fig. 6. Given that surface quality plays a significant role

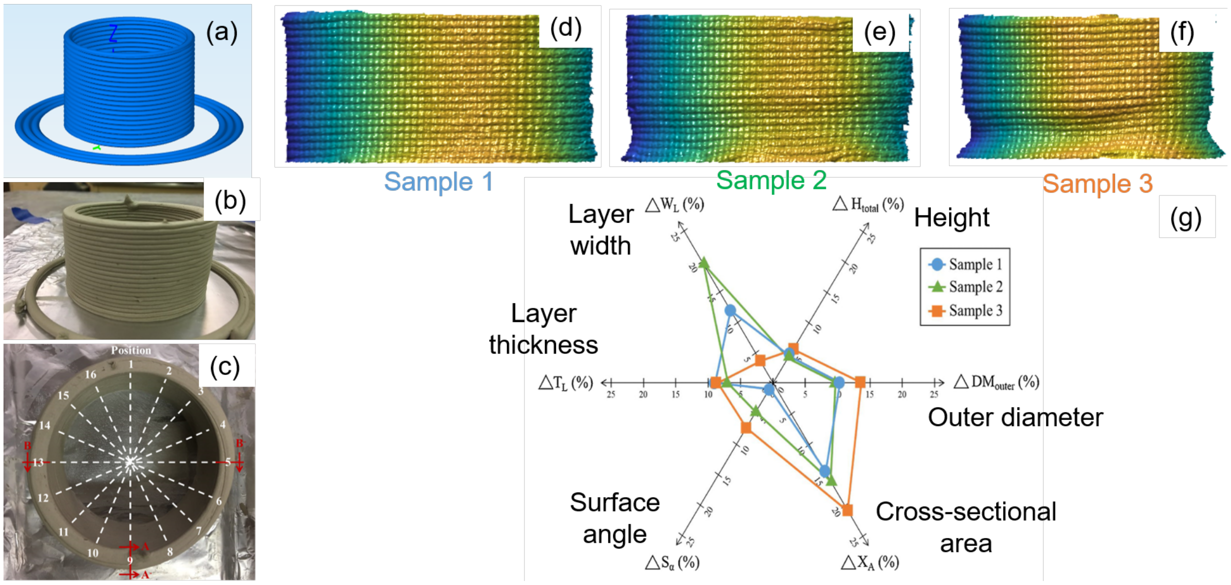

Figure 5. An example of morphological data analysis using 3D optical sensing data for clay additive printing. (a) The 3D solid model for the printing structure; (b) - (c) side and top views of the printed structure; (d) - (f) side view of the reconstructed 3D geometry data for three different printed samples with different printing configurations; (g) the contour plots of different dimensional features of the printed samples. This picture is reprinted with permission from Reference [48]. Copyright Elsevier (2020).

on determining the functionality and durability of manufactured products, providing meaningful surface characterization can be extremely important for surface engineering given that it can provide a better understanding of the relationship between the surface processing parameters and the properties of the corresponding surface finishes.

Table 1 illustrates a set of parameters that are useful in characterizing the areal roughness properties of a manufactured surface finish. The top five rows are the basic areal roughness parameter that describes the arithmetical mean height (S_a), root mean square height (S_q), maximum peak height (S_p), maximum valley height (S_v), and maximum height ($S_z = S_p + S_v$) which are very intuitive from its definition. The last two rows are parameters that describe the distributions of a surface. Specifically, the skewness value (Ssk) indicates the deviation of the height distribution against the mean plane. A positive Ssk means the height distribution is skewed above the mean plane, while a negative Ssk means the height distribution is skewed below the mean plane. Such value will depict whether the surface is predominated by peaks or valleys, as shown in Fig. 7(a). On the other hand, the kurtosis value (Sku) indicates the sharpness of the peaks and valleys. As shown in Fig 7(b), a Sku value above 3 means that the surface is dominated by sharp peaks or valleys, yet a Sku value below 3 means that the surface exhibits blunt peaks and valleys. These surface roughness parameters can serve as important indicators for process enhancement and control to improve surface integrity.

4. Summary

This paper has presented the advances in high-speed 3D optical sensing technology and its applications to manufacturing research. A specific focus was set on the fringe projection technique as the most suitable method for simultaneous high-speed and high-accuracy 3D shape measurements. Some representative measurement examples were presented to introduce the applications of high-speed 3D optical sensing on

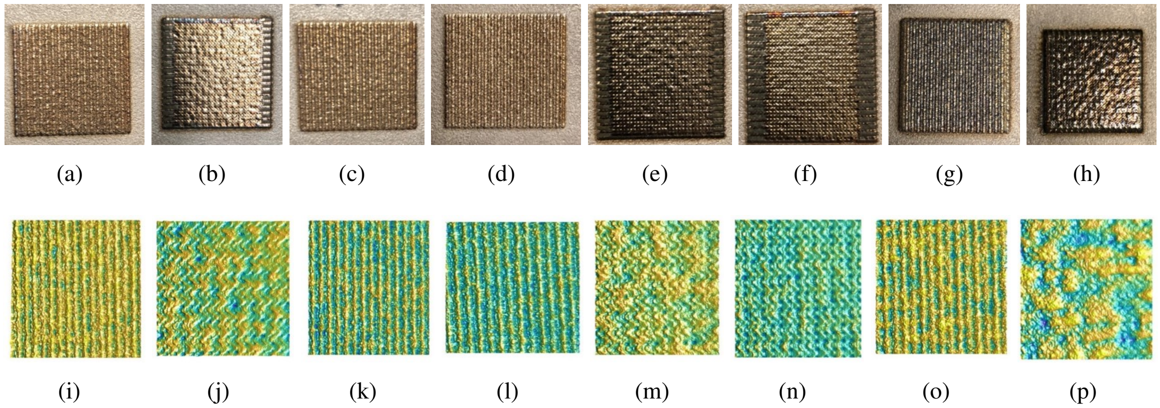

Figure 6. Examples of additive manufactured surfaces with different surface topographies. (a) - (h) Photographs of the manufactured surfaces; (i) - (p) corresponding reconstructed surface topographies.

Table 1. Areal surface roughness parameters.

Notation	Physical meaning	Equation
S_a	Arithmetical mean height	$\frac{1}{A}\iint_A \lvert z(x,y)\rvert dxdy$
S_q	Room mean square height	$\sqrt{\frac{1}{A}\iint_A \lvert z^2(x,y)\rvert dxdy}$
S_p	Maximum peak height	$\lvert \max_A z(x,y)\rvert$
S_v	Maximum valley height	$\lvert \min_A z(x,y)\rvert$
S_z	Maximum height	$S_p + S_v$
Ssk	Skewness	$\frac{1}{S_q^2}\iint_A z^3(x,y)dxdy$
Sku	Kurtosis	$\frac{1}{S_q^4}\iint_A z^4(x,y)dxdy$

both in-situ process monitoring and post-process quality assessments. The author hopes this paper will introduce the potential applications of the fringe-projection-based high-speed 3D optical sensing technology to the manufacturing community.

Acknowledgments

The author would like to thank his former/current students (Dr. Vignesh Suresh, Dr. Yi Zheng, Mr. Weijun Shen, and Mr. Li-Hsin Yeh) and his research collaborators (Dr. Yiliang Liao, Dr. Minghui Zheng, Dr. Kejin Wang, and Dr. Hantang Qin) for their valuable suggestions and contributions. This research was funded by National Science Foundation Directorate for Engineering (CMMI-2132773). The views expressed here are those of the authors and are not necessarily those of the NSF.

Funding: National Science Foundation Directorate for Engineering (CMMI-2132773).

Disclosure statement: The author declares no conflict of interest.

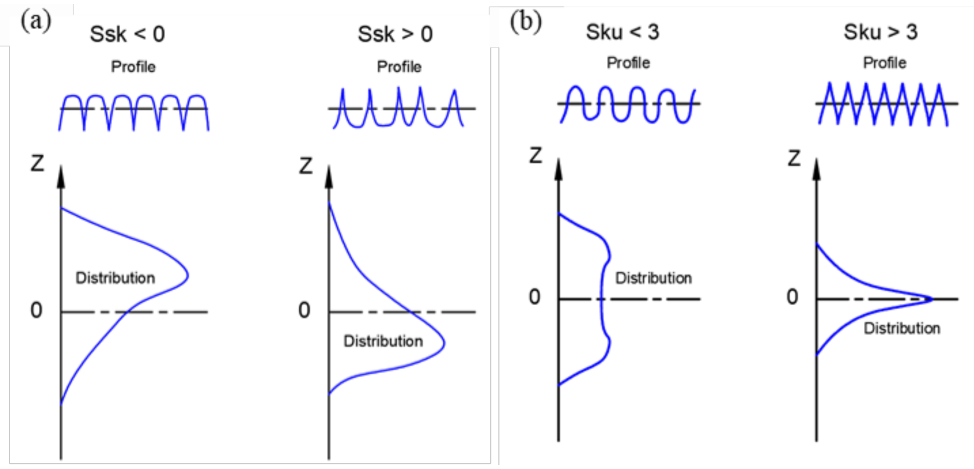

Figure 7. Graphical representation of the physical meaning of (a) skewness Ssk and (b) kurtosis Sku.

References

[1] Arkadeep Kumar. Methods and materials for smart manufacturing: additive manufacturing, internet of things, flexible sensors and soft robotics. *Manufacturing Letters*, 15:122–125, 2018.

[2] Yuhang Yang, Zhiqiao Dong, Yuquan Meng, and Chenhui Shao. Data-driven intelligent 3d surface measurement in smart manufacturing: review and outlook. *Machines*, 9(1):13, 2021.

[3] Longyu Zhang, Haiwei Dong, and Abdulmotaleb El Saddik. From 3d sensing to printing: A survey. *ACM Transactions on Multimedia Computing, Communications, and Applications (TOMM)*, 12(2):1–23, 2015.

[4] QMJ Qu, MF Ricky Lee, and Clarence W de Silva. Intelligent 3d sensing in automated manufacturing processes. In *2001 IEEE/ASME International Conference on Advanced Intelligent Mechatronics*, volume 1, pp. 366–370. IEEE, 2001.

[5] Kevin Harding. *Handbook of optical dimensional metrology*. CRC Press, 2013.

[6] Toru Yoshizawa. *Handbook of optical metrology: Principles and Applications*. CRC press, 2009.

[7] W Gao, H Haitjema, FZ Fang, RK Leach, CF Cheung, E Savio, and Jean-Marc Linares. On-machine and in-process surface metrology for precision manufacturing. *CIRP Annals*, 68(2):843–866, 2019.

[8] Sarah K Everton, Matthias Hirsch, Petros Stravroulakis, Richard K Leach, and Adam T Clare. Review of in-situ process monitoring and in-situ metrology for metal additive manufacturing. *Materials & Design*, 95:431–445, 2016.

[9] Sai Siva Gorthi and Pramod Rastogi. Fringe projection techniques: whither we are? *Optics and Lasers in Engineering*, 48(2):133–140, 2010.

[10] Jason Geng. Structured-light 3d surface imaging: a tutorial. *Advances in Optics and Photonics*, 3(2):128–160, 2011.

[11] Andres G Marrugo, Feng Gao, and Song Zhang. State-of-the-art active optical techniques for three-dimensional surface metrology: a review [invited]. *Journal of the Optical Society of America A*, 37(9):B60–B77, 2020.

[12] Samuel Tolansky. *An introduction to interferometry*. Longman, 1973.

[13] James C Wyant. White light interferometry. In *Holography: A Tribute to Yuri Denisyuk and Emmett Leith*, volume 4737, pp. 98–107. SPIE, 2002.

[14] James C Wyant. Interferometric optical metrology: Basic principles and new systems. *Laser Focus, USA*, 18(5):65–71, 1982.

[15] Andreas Kolb, Erhardt Barth, Reinhard Koch, and Rasmus Larsen. Time-of-flight cameras in computer graphics. *Computer Graphics Forum*, 29(1):141–159, 2010.

[16] Filiberto Chiabrando, Roberto Chiabrando, Dario Piatti, and Fulvio Rinaudo. Sensors for 3d imaging: Metric evaluation and calibration of a ccd/cmos time-of-flight camera. *Sensors*, 9(12):10080–10096, 2009.

[17] Robert Lange and Peter Seitz. Solid-state time-of-flight range camera. *IEEE Journal of Quantum Electronics*, 37(3):390–397, 2001.

[18] Yan Cui, Sebastian Schuon, Derek Chan, Sebastian Thrun, and Christian Theobalt. 3d shape scanning with a time-of-flight camera. In *Proc. IEEE on CVPR*, pp. 1173–1180. IEEE, 2010.

[19] Carlo Dal Mutto, Pietro Zanuttigh, and Guido M Cortelazzo. *Time-of-flight cameras and Microsoft Kinect (TM)*. Springer Science & Business Media, 2012.

[20] S Parthasarathy, J Birk, and J Dessimoz. Laser rangefinder for robot control and inspection. In *Robot Vision*, volume 336, pp. 2–11. SPIE, 1982.

[21] G Bickel, G Hausler, and M Maul. Triangulation with expanded range of depth. *Optical Engineering*, 24(6):246975, 1985.

[22] João Guilherme DM França, Mário A Gazziro, Alessandro Noriaki Ide, and José Hiroki Saito. A 3d scanning system based on laser triangulation and variable field of view. In *IEEE International Conference on Image Processing 2005*, volume 1, pp. I–425. IEEE, 2005.

[23] Rainer G Dorsch, Gerd Häusler, and Jürgen M Herrmann. Laser triangulation: fundamental uncertainty in distance measurement. *Applied Optics*, 33(7):1306–1314, 1994.

[24] Umesh R Dhond and Jake K Aggarwal. Structure from stereo-a review. *IEEE transactions on systems, man, and cybernetics*, 19(6):1489–1510, 1989.

[25] Daniel Scharstein and Richard Szeliski. A taxonomy and evaluation of dense two-frame stereo correspondence algorithms. *International Journal of Computer Vision*, 47(1):7–42, 2002.

[26] Joaquim Salvi, Jordi Pages, and Joan Batlle. Pattern codification strategies in structured light systems. *Pattern Recognition*, 37(4):827–849, 2004.

[27] Song Zhang. Recent progresses on real-time 3-d shape measurement using digital fringe projection techniques. *Optics and Lasers in Engineering*, 48(2):149–158, 2010.

[28] Sam Van der Jeught, Joris AM Soons, and Joris JJ Dirckx. Real-time microscopic phase-shifting profilometry. *Applied Optics*, 54(15):4953–4959, 2015.

[29] Nikolaus Karpinsky, Morgan Hoke, Vincent Chen, and Song Zhang. High-resolution, real-time three-dimensional shape measurement on graphics processing unit. *Optical Engineering*, 53(2):024105, 2014.

[30] Song Zhang. *High-speed 3D imaging with digital fringe projection techniques*. CRC Press, 2018.

[31] Mitsuo Takeda, Hideki Ina, and Seiji Kobayashi. Fourier-transform method of fringe-pattern analysis for computer-based topography and interferometry. *Journal of the Optical Society of America A*, 72(1):156–160, 1982.

[32] Daniel Malacara. *Optical shop testing*, volume 59. John Wiley & Sons, 2007.

[33] Song Zhang. Absolute phase retrieval methods for digital fringe projection profilometry: A review. *Optics and Lasers in Engineering*, 107:28–37, 2018.

[34] Chao Zuo, Lei Huang, Minliang Zhang, Qian Chen, and Anand Asundi. Temporal phase unwrapping algorithms for fringe projection profilometry: A comparative review. *Optics and Lasers in Engineering*, 85:84–103, 2016.

[35] Beiwen Li, Nikolaus Karpinsky, and Song Zhang. Novel calibration method for structured-light system with an out-of-focus projector. *Applied optics*, 53(16):3415–3426, 2014.

[36] Shuangyan Lei and Song Zhang. Flexible 3-d shape measurement using projector defocusing. *Optics Letters*, 34(20):3080–3082, 2009.

[37] Shijie Feng, Liang Zhang, Chao Zuo, Tianyang Tao, Qian Chen, and Guohua Gu. High dynamic range 3d measurements with fringe projection profilometry: a review. *Measurement Science and Technology*, 29(12):122001, 2018.

[38] Hui Lin, Jian Gao, Guanjin Zhang, Xin Chen, Yunbo He, and Yan Liu. Review and comparison of high-dynamic range three-dimensional shape measurement techniques. *Journal of Sensors*, 2017, 2017.

[39] Yue Liu, Liam Blunt, Feng Gao, and Xiangqian Jiang. High-dynamic-range 3d measurement for e-beam fusion additive manufacturing based on svm intelligent fringe projection system. *Surface Topography: Metrology and Properties*, 9(3):034002, 2021.

[40] Liang Zhang, Qian Chen, Chao Zuo, and Shijie Feng. High-speed high dynamic range 3d shape measurement based on deep learning. *Optics and Lasers in Engineering*, 134:106245, 2020.

[41] Bin Zhang, John Ziegert, Faramarz Farahi, and Angela Davies. In situ surface topography of laser powder bed fusion using fringe projection. *Additive Manufacturing*, 12:100–107, 2016.

[42] Andrew Dickins, Taufiq Widjanarko, Danny Sims-Waterhouse, Adam Thompson, Simon Lawes, Nicola Senin, and Richard Leach. Multi-view fringe projection system for surface topography measurement during metal powder bed fusion. *Journal of the Optical Society of America A*, 37(9):B93–B105, 2020.

[43] Haolin Zhang, Chaitanya Krishna Prasad Vallabh, Yubo Xiong, and Xiayun Zhao. A systematic study and framework of fringe projection profilometry with improved measurement performance for in-situ lpbf process monitoring. *Measurement*, 191:110796, 2022.

[44] Zhongwei Li, Xingjian Liu, Shifeng Wen, Piyao He, Kai Zhong, Qingsong Wei, Yusheng Shi, and Sheng Liu. In situ 3d monitoring of geometric signatures in the powder-bed-fusion additive manufacturing process via vision sensing methods. *Sensors*, 18(4):1180, 2018.

[45] Xiao Zhang, Weijun Shen, Vignesh Suresh, Jakob Hamilton, Li-Hsin Yeh, Xuepeng Jiang, Zhan Zhang, Qing Li, Beiwen Li, Iris V Rivero, et al. In situ monitoring of direct energy deposition via structured light system and its application in remanufacturing industry. *The International Journal of Advanced Manufacturing Technology*, 116(3):959–974, 2021.

[46] Giovanna Sansoni, Matteo Carocci, and Roberto Rodella. Three-dimensional vision based on a combination of gray-code and phase-shift light projection: analysis and compensation of the systematic errors. *Applied Optics*, 38(31):6565–6573, 1999.

[47] Beiwen Li and Song Zhang. Flexible calibration method for microscopic structured light system using telecentric lens. *Optics Express*, 23(20):25795–25803, 2015.

[48] Kwangwoo Wi, Vignesh Suresh, Kejin Wang, Beiwen Li, and Hantang Qin. Quantifying quality of 3d printed clay objects using a 3d structured light scanning system. *Additive Manufacturing*, 32:100987, 2020.